Check for updates

View Article Online
View Journal

Analyst

Accepted Manuscript

This article can be cited before page numbers have been issued, to do this please use: R. Zhang, J. zhang, X. Qu, S. Li, Y. Zhao, S. Liu, Y. Wang, J. Huang and J. Yu, *Analyst*, 2020, DOI: 10.1039/D0AN00139B.

This is an Accepted Manuscript, which has been through the Royal Society of Chemistry peer review process and has been accepted for publication.

Accepted Manuscripts are published online shortly after acceptance, before technical editing, formatting and proof reading. Using this free service, authors can make their results available to the community, in citable form, before we publish the edited article. We will replace this Accepted Manuscript with the edited and formatted Advance Article as soon as it is available.

You can find more information about Accepted Manuscripts in the Information for Authors.

Please note that technical editing may introduce minor changes to the text and/or graphics, which may alter content. The journal's standard Terms & Conditions and the Ethical guidelines still apply. In no event shall the Royal Society of Chemistry be held responsible for any errors or omissions in this Accepted Manuscript or any consequences arising from the use of any information it contains.

View Article Online
DOI: 10.1039/D0AN00139B

Efficient strand displacement amplification via stepwise movement of bipedal DNA walker on electrode surface for ultrasensitive detection of antibiotic

Rufeng Zhang[a], Jie Zhang[a], Xiaonan Qu[a], Shasha Li[b], Yihan Zhao[b],

Su Liu[a], Yu Wang[b] Jiadong Huang[b c] Jinghua Yu[c]*

a School of Water Conservancy and Environment, University of Jinan, Jinan 250022,P.R. China.

b College of Biological Scaiences and Technology, University of Jinan, Jinan 250022, P.R. China.

c Key Laboratory of Chemical Sensing & Analysis in Universities of Shandong, College of Chemistry and Chemical Engineering, University of Jinan, Jinan 250022, P.R. China.

Published on 11 February 2020. Downloaded by University of Newcastle on 2/12/2020 9:10:41 AM.

Analyst Accepted Manuscript

View Article Online
DOI: 10.1039/D0AN00139B

* Corresponding author. E-mail: stu_lius@ujn.edu.cn; Tel.: +86-531-89736122; Fax: +86-531-82769122.

Published on 11 February 2020. Downloaded by University of Newcastle on 2/12/2020 9:10:41 AM.

Analyst Accepted Manuscript

View Article Online
DOI: 10.1039/D0AN00139B

Published on 11 February 2020. Downloaded by University of Newcastle on 2/12/2020 9:10:41 AM.

Abstract

DNA walkers, one of the artificial molecular machines which are constructed via smart synthetic DNA, have attracted rapidly growing attention of researchers in biosensing fields. In this work, we design an Exonuclease III (Exo III)-aided target-aptamer binding recycling (ETBR) activated bipedal DNA machine for highly sensitive electrochemical detection of antibiotic. To the best of our knowledge, this is the first time that the bipedal DNA machine has been applied in electrochemical sensing for antibiotics. On the one hand, the bipedal DNA walker exceeds the conventional single swing arm DNA walker in terms of walking efficiency and stability. On the other hand, ETBR strategy, along with the efficient strand displacement amplification via stepwise movement of bipedal DNA walker significantly promotes the signal amplification efficiency. Under optimal conditions, this bipedal DNA machine possesses a detection limit to 7.1 fM within a linear detection range from 10 fM to 100 pM. Moreover, this electrochemical biosensor is expected to detect wide variety of analytes by using corresponding target recognition probes. Thus, our proposed strategy offers a highly efficient, stable and practical platform for small molecule analysis.

Keywords: Bipedal DNA walker; strand displacement amplification; electrochemical biosensor; antibiotic

Analyst Accepted Manuscript

View Article Online
DOI: 10.1039/D0AN00139B

1. Introduction

Antibiotics, as an effective medicine, are widely applied in inhibiting the growth and reproduction of bacteria.[1] Nevertheless, the misuse of antibiotics will inevitably lead to antibiotic residue and negative effects, such as nephrotoxicity, allergic reactions and antibiotic resistance.[2-4] Therefore, developing a rapid and efficient strategy for the detection of antibiotics in the water and foodstuffs is highly advisable.

Nowadays, scholars have exploited multiple instrumental methods to quantify residual antibiotics, such as high performance liquid chromatography (HPLC),[5] surface-enhanced Raman scattering (SERS),[6, 7] surface plasmon resonance (SPR).[8-10] However, these instrumental methods have inherent disadvantages such as poor specificity, expensive equipment and complicated operation. Thus, it is of great research significance to develop a fast and efficient method for quantitative analysis of antibiotics.

In this context, a variety of colorimetric,[11-13] fluorescent,[14-16] electrochemical biosensors[17-19] have been applied for the detection of antibiotics and other biomolecules. To improve the sensitivity, many signal amplification strategies including the hybridization chain reaction (HCR)[20-22], rolling circle amplification (RCA)[23, 24], catalyzed hairpin assembly (CHA)[25, 26] and DNA walking machine[27-29] have been developed. Among them, DNA walking machines, one of the artificial molecular machines, as the ingenious dynamic interaction and capabilities for signal amplification have been widely integrated into electrochemical biosensing fields. This

Published on 11 February 2020. Downloaded by University of Newcastle on 2/12/2020 9:10:41 AM.

Analyst Accepted Manuscript

View Article Online
DOI: 10.1039/D0AN00139B

is not only because of the advantages of high sensitivity, low cost, and flexible operation of electrochemical strategies, but also the electrodes provide a stable and suitable interface for DNA machines. For example, Chen et al proposed a one-step electrochemical DNA walker for proteins identification based on target-induced proximity recognition.[30] Cai's group designed an electrochemical platform through using DNA walker as signal amplification method for the detection of breast cancer cell[31]. However, above DNA machine employed the single swing arm as assembly operation which the walking efficiency will be restricted. To address this problem, some bipedal DNA walker methods were constructed to improve the walking efficiency[32]. For instance, Yang's group designed a bipedal DNA walker via simultaneous binding of two DNA linked-affinity ligands for sensing thrombin.[33] Although bipedal DNA machine can improve walking efficiency to a certain degree, the conventional strategy of a target generated only one DNA walker limited the total number of DNA walkers and their walking speed.

In response, we report an efficient strand displacement amplification method by stepwise movement of bipedal DNA walker on the electrode for ultrasensitive detection of antibiotic. To the best of our knowledge, this is the first time that the bipedal DNA machine has been utilized for electrochemical sensing for antibiotics. This proposed strategy features with several aspects. Firstly, ETBR can output countless DW in comparison to the previous way of a target generates only one DNA walker. Secondly, bipedal DNA walker can not only improve amplification

Published on 11 February 2020. Downloaded by University of Newcastle on 2/12/2020 9:10:41 AM.

Analyst Accepted Manuscript

View Article Online
DOI: 10.1039/D0AN00139B

efficiency, but also obviously enhance stability and walking efficiency by simultaneous combining two DNA capture probes. Additionally, by replacing antibiotic aptamer by the corresponding DNA substrates for target recognition, this bipedal DNA machine can readily enable the detection of various targets. Therefore, this electrochemical biosensor provides a stable, universal and efficient method for ultrasensitive antibiotics detection and other molecules with trace amounts in bioanalysis.

2. Experimental

2.1. Reagents and materials

All the antibiotics used in the experiment and 6-mercapto-l-hexanol (MCH) were bought from Aladdin Chemistry Co. Ltd (Shanghai, China). All oligonucleotides were HPLC-purified and synthesized by Sangon Biotechnology Co. Ltd (Shanghai, China). The oligonucleotide sequences were listed in **Table 1**. All other chemical reagents were purchased from Sinopharm Chemical Reagent Co. Ltd (Beijing, China). All solutions were prepared using ultrapure water with an electric resistance of >18.25 MΩ cm obtained through a Millipore Milli-Q water purification system (Billerica, MA, USA). Phosphate Buffered Saline (PBS, 10 mM PB, 0.14 M NaCl, pH 7.4) was used during the experiments. Before the experiment, the S1, S2 and CP were mixed to form S1-S2-CP complex at 95 °C for 5 min and cooled to indoor temperature.

Table 1 Oligonucleotides sequences used in this study.

Published on 11 February 2020. Downloaded by University of Newcastle on 2/12/2020 9:10:41 AM.

Analyst Accepted Manuscript

View Article Online
DOI: 10.1039/D0AN00139B

Oligonucleotide name	Sequence (5' to 3') description
Hairpin probe 1(HP1)	TAGCCTTTTTTTGGGGGTTGAGGCTAAGCCGAC
Hairpin probe 2 (HP2)	*TTTTTTCATACCTTTATCAGTACCTCTCTATTACACTTTTT TCATACC*TACTGATAAAGGTATGAAAAAAGGCTA
S1	GTCATTCAATCAAGGTGTGCATCTTTT
S2	CGATCGTTTTTTTTT
Capture probe (CP)	GGTATGAAAAAACGATCGGATGCACACCTTGATTG AATGACATATAT-SH
Signal probe (SP)	MB-GTCATTCAATCAAGGTGTGCTCCGATCGTTTTTT CATTTT

The underlined of HP1 is the kanamycin aptamer. The italic of HP2 is the sequence of BW.

2.2 Apparatus and measurements

Cyclic voltammetry (CV), differential pulse voltammetry (DPV) and electrochemical impedance spectroscopy (EIS) were measured with a CHI660D electrochemical workstation bought from Shanghai Huachen Instrument Co. Ltd. We used a classical three-electrode system which consisted of an Ag/AgCl electrode as the reference electrode, platinum wire as the auxiliary electrode and a gold electrode with a diameter of 2 mm as the working electrode. CV and EIS were performed in 5

Published on 11 February 2020. Downloaded by University of Newcastle on 2/12/2020 9:10:41 AM.

Analyst Accepted Manuscript

View Article Online
DOI: 10.1039/D0AN00139B

mM $[Fe(CN)_6]^{3-/4-}$ containing 0.25 M KCl. DPV was performed in PBS (10 mM, pH 7.4) in the voltage range from 0 to -0.5 V.

2.3 Gold electrode treatment and modification

The working electrodes were polished carefully with 0.3 and 0.05 mm alumina suspension. Next, the gold electrodes were immersed in a freshly prepared piranha solution (H_2O_2/H_2SO_4, the volume ratio was 1:3) for 2 h, and then rinsed using ultrapure water thoroughly. Immediately, the gold electrodes were cleaned with ultrasonication in ethanol solution. Then, in the process of electrode modification, 3 μL pure of 10 μM the mixture solution S1-S2-CP was modified on the gold electrode via the Au-S bond for 2 h at 37°C. Then, the electrodes were rinsed using PBS to wipe off the unabsorbed S1-S2-CP. Thereafter, the gold electrodes were immersed into a 2 mM MCH solution for 1 h to block the unoccupied sites of the electrode and eliminate nonspecific adsorption. Finally, the working electrodes were completely rinsed with PBS and stored at 4°C.

2.4. Kanamycin detection

The details of the experiment were as follows: Sample solution of 10 μL kanamycin (the final concentrations ranging from 0 to 100 pM), 3 μL pure of 10 nM (final concentration) HP1, 3 μL pure of 500 nM (final concentration) HP2, 2 μL 10×NEBuffer and 2 μL Exo III were mixed at 37°C for 2 h to perform the Exo III-assisted target-aptamer binding recycle. Subsequently, the 20 μL aforementioned solution together with 3 μL pure of 10 μM SP were added to the surface of Au

Published on 11 February 2020. Downloaded by University of Newcastle on 2/12/2020 9:10:41 AM.

Analyst Accepted Manuscript

View Article Online
DOI: 10.1039/D0AN00139B

electrode and incubated in a humid atmosphere at 37 °C for 2 h. Next, the gold electrode was completely rinsed with 1×PBS for three times. Finally, the DPV signal of the biosensor was collected in 15 mL of PBS (10 mM, pH 7.4).

3. Results and discussion

3.1 Principle of the proposed electrochemical biosensor strategy

The detection principle of bipedal DNA machine is depicted in **Scheme 1**. Kanamycin is used as a model analyte. This bipedal DNA machine contains a DNA modified electrochemical sensing interface, namely S1-S2-CP, hairpin probe 1 (HP1) containing the kanamycin aptamer sequence, hairpin probe 2 (HP2), a signal probe (SP) labeled with methylene blue (MB) and Exo III. To achieve high sensitivity and specificity for antibiotics quantification, Exo III-aided target-aptamer binding recycling (ETBR) is used as the first stage of signal amplification. When the target is present, target specifically binds the HP1 and change its conformational, the target-HP1 complex anneal with the protruding tail of HP2 forming DNA duplex with a blunt 3'-terminus. Immediately, Exo III recognizes the duplex and catalyzes the stepwise removal of mononucleotides from the blunt 3' end of HP2 in the 3' to 5' direction, which induces the generation of bipedal walker (BW) and the release of target-HP1. Simultaneously, free target-HP1 continues to hybridize with another HP2, initiating a new cycle. After ETBR process, a mass of BW can be produced in the solution. Subsequently, the resulting BW is dropped on electrode surfaces for efficient strand displacement amplification and electrochemical sensing. The bipedal DNA

Published on 11 February 2020. Downloaded by University of Newcastle on 2/12/2020 9:10:41 AM.

Analyst Accepted Manuscript

View Article Online
DOI: 10.1039/D0AN00139B

machine is activated with the combination of BW and CP, while releases S1. Ulteriorly, SP interacts with CP and leads to the release of S2, accompanying in the complete hybridization of CP and SP concurrent restoration of initially BW. Meanwhile, the free BW moves autonomously upon combining with surplus CP, accordingly, numerous SP gathered on electrode surfaces and a dramatically strong DPV signal is obtained due to the reduction of MB. In summary, the electrochemical biosensor provides a stable, universal and efficient strategy for kanamycin identification and related small molecule analysis.

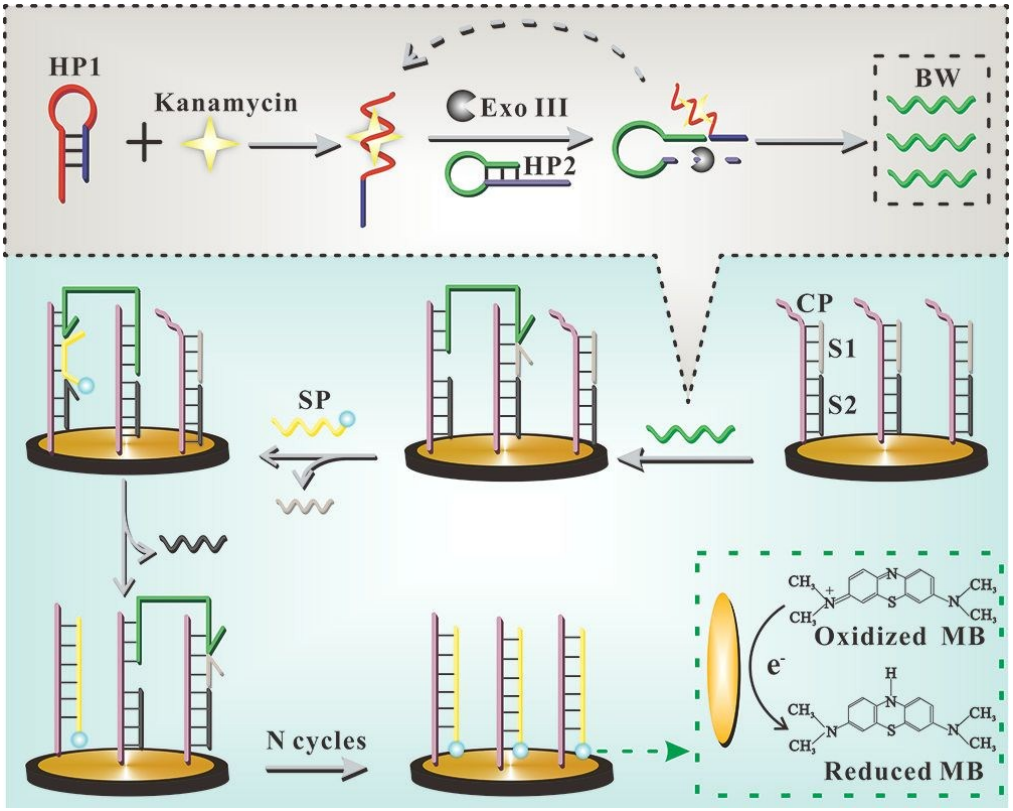

Scheme 1. Schematic illustration of the biosensor for kanamycin detection.

3.2 Feasibility analysis of bipedal DNA machine

To confirm the feasibility of our bipedal DNA machine, a series of control

Published on 11 February 2020. Downloaded by University of Newcastle on 2/12/2020 9:10:41 AM.

Analyst Accepted Manuscript

View Article Online
DOI: 10.1039/D0AN00139B

Published on 11 February 2020. Downloaded by University of Newcastle on 2/12/2020 9:10:41 AM.

experiments were investigated, and these results were displayed in **Fig.1**. For the positive sample, a significantly strong DPV signal was obtained (curve a), indicating that numerous SP combined to the CP on the electrode and accelerated the electron transfer between the electrode and MB. In contrast, it was found a negligible current signal for the blank sample (curve b). This result proved the activation of DNA machine relied on the specific kanamycin-aptamer interaction. When there is no Exo III in the reaction solution, we observed a slightly weaker electrochemical response (curve c), implying Exo III was essential for the operation of bipedal DNA walker. In addition, when kanamycin was replaced by terramycin, a low DPV response similar to the blank sample was collected (curve d), which proved the high specificity of this electrochemical biosensor for kanamycin detection.

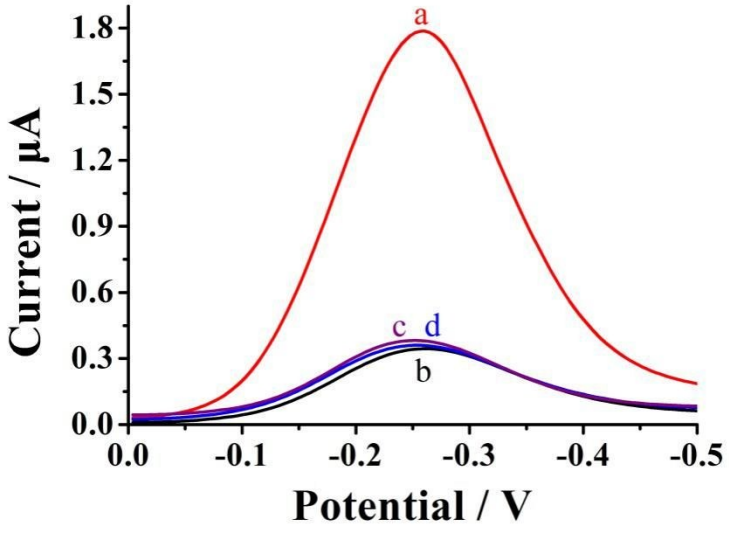

Fig.1. DPV signal of the electrochemical DNA machine collected by analyzing 100 pM kanamycin (a). Curves b to d were for the control experiments which were performed with blank sample (b), 100 pM kanamycin without Exo III (c), kanamycin

Analyst Accepted Manuscript

View Article Online
DOI: 10.1039/D0AN00139B

was replaced by 100 pM non-target terramycin (d).

3.3 Electrochemical characterization of the modified electrodes

Fabrication of the bipedal DNA machine was further verified by cyclic voltammetry (CV), electrochemical impedance spectroscopy (EIS), respectively. As depicted in Figure 2A, a pair of well-defined current peaks was obtained for bare Au electrode (curve a). Since negatively charged oligonucleotides could repel $[Fe(CN)_6]^{3-/4-}$, the peaks weakened after the immobilization of S1-S2-CP (curve b). After being blocked with MCH, there was a decreased redox current (curve c), which was attributed that the nonconductive property of MCH was able to impede the electron transfer on electrode surfaces. After the incubation of the modified electrode with kanamycin, the redox current showed noticeable decrease (curve d), suggesting the bipedal DNA machine was activated. Further, after the incubation of the aforementioned electrode with SP, the peak current had a significant increase (curve e), proving SP facilitated the release of BW. All of the above data indicated the fabrication process of the electrochemical sensing interface. Similarly, EIS results were also recorded and summarized the fabrication procedure of the DNA machine in Figure 2B. As shown in Figure 2B, the bare Au electrode showed a greatly small electron transfer resistance (Ret) (curve a). After the immobilization of S1-S2-CP on electrode surface, the Ret displayed a substantial increase, manifesting the negatively charged phosphate backbone excluded the electron transfer on electrode surfaces (curve b). Since the non-specific sites were blocked by MCH, the Ret continued to

Published on 11 February 2020. Downloaded by University of Newcastle on 2/12/2020 9:10:41 AM.

Analyst Accepted Manuscript

View Article Online
DOI: 10.1039/D0AN00139B

increase (curve c). Additionally, with the incubation of kanamycin, the Ret exhibited an obvious increase (curve d), certifying the bipedal DNA walker had been assembled. Next, after the incubation of the modified electrode with SP, there was a certainly decrease for Ret due to SP combined CP to induce the free of BW. The EIS changes were agreement with the CV responses, which forceful described the preparation process of the electrochemical DNA machine interface.

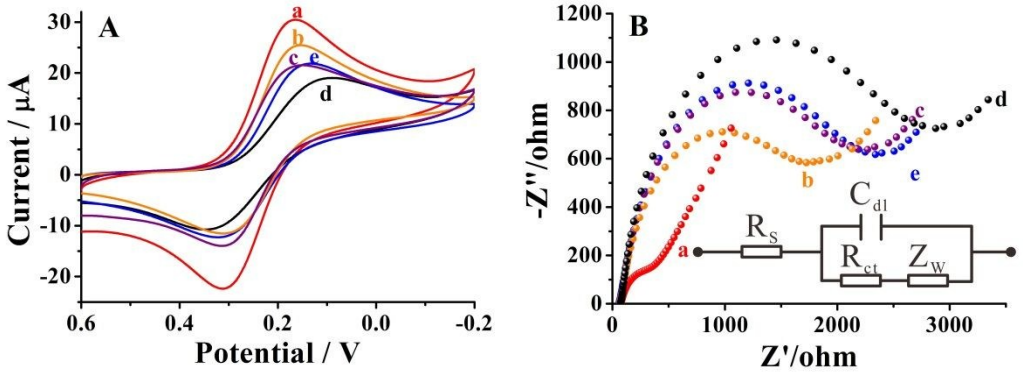

Fig.2. (A) CVs and (B) EIS described for the bare Au electrode (a), CP-S1-S2/Au (b), MCH/CP-S1-S2/Au (c), kanamycin/MCH/CP-S1-S2/Au (d), kanamycin/SP/MCH/ CP-S1-S2/Au (e). CV and EIS measurements were performed in containing 0.25 mM KCl and 5.0 mM $K_3[Fe(CN)_6]$

3.4 Optimization of the experimental conditions

To achieve optimal performance for kanamycin detection by electrochemical biosensor, the experimental conditions, including homogeneous reaction time, the concentration of Exo III and the molar ratio of HP2 and CP were researched. As shown in Fig. 3A, it was observed that the DPV peak intensities for the positive sample enhanced continuously with increasing of the reaction time until a plateau was

Published on 11 February 2020. Downloaded by University of Newcastle on 2/12/2020 9:10:41 AM.

Analyst Accepted Manuscript

View Article Online
DOI: 10.1039/D0AN00139B

reached at 2 h (curve a). In contrast, for blank sample, there was almost no visible change in current intensity (curve b). Thus, 2 h was chosen as the optimized homogeneous reaction time in the following experiments. In addition, the concentration of Exo III was essential for the current responses of the bipedal DNA machine. As depicted in the Fig. 3B, we researched the relationship between the concentration of Exo III and the $(I_1-I_0)/I_0$ values. I_1 and I_0 represent the DPV signal in the presence and absence of 100 pM kanamycin, respectively. In Fig. 3B, the $(I_1-I_0)/I_0$ increased with an increase in the concentration of Exo III and became saturated after 10 U; so, we selected 10 U as the optimal concentration for Exo III. In the Fig. 3C, the current peak intensities gradually increased with the augment of the molar ratios and reached a maximum intensity when the ratio of HP2 and CP was 1:20. Once beyond the ratio of 1:20, the current intensities reduced upon an increase of the ratio. For the blank sample, the current peak intensities displayed no obvious increase with increasing of the molar ratios. So, 1:20 was used as the subsequent experiments.

Published on 11 February 2020. Downloaded by University of Newcastle on 2/12/2020 9:10:41 AM.

Analyst Accepted Manuscript

View Article Online
DOI: 10.1039/D0AN00139B

Published on 11 February 2020. Downloaded by University of Newcastle on 2/12/2020 9:10:41 AM.

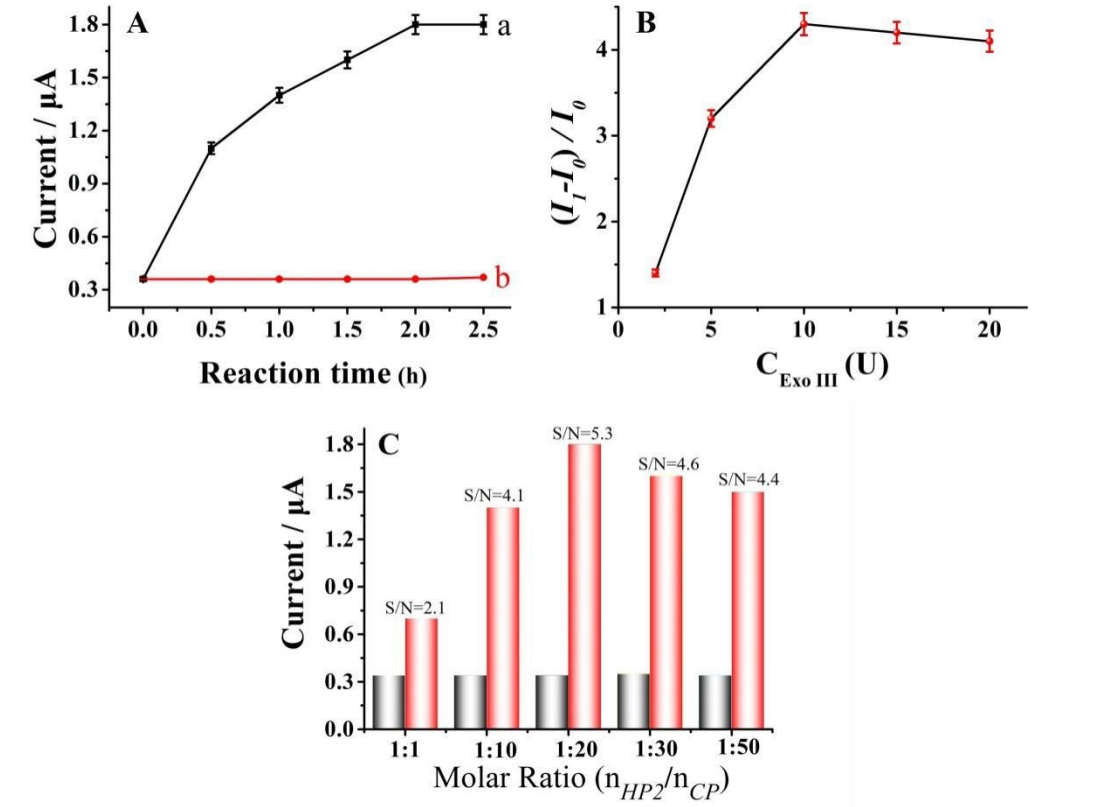

Fig.3. (A) Effect of the homogeneous reaction time on the DPV signal intensity of the biosensor in the presence (curve a) and absence (curve b) of 100 pM kanamycin; (B) Effect of the concentration Exo III to the DPV peak intensities of the bipedal DNA machine; (C) Effect of the molar ratio of HP2 and CP to current peak of the bipedal DNA machine in the presence (the red bar) and absence (the black bar) of 100 pM kanamycin. Error bars were standard deviations across three repetitive experiments.

3.5 Analytical performance of the electrochemical biosensor for detecting kanamycin

Under the above-mentioned optimized experimental conditions, the analytical performance of the electrochemical biosensor was investigated towards the detection of kanamycin at various concentrations. As seen from Fig. 4A, the DPV intensity

Analyst Accepted Manuscript

View Article Online
DOI: 10.1039/D0AN00139B

increased with increasing kanamycin concentration from 0 to 100 pM. The plot of the DPV peak intensities versus the logarithm value of kanamycin concentrations showed an excellent linear dependence in the range from 10 fM to 100 pM (inset in Fig. 4B), and the calibration equation was calculated to be I (μA) = 0.11+ 0.33 lg($C_{kanamycin}$ /fM) with the correlation coefficient of 0.994. The limit of detection (LOD) was calculated to be 7.1 fM in terms of the rule of 3 times standard deviation of the blank divided by the slope of the calibration line. Furthermore, we compared this bipedal DNA machine with previous reported methods of quantitative assay of kanamycin and the results were shown in **Table 2**. It was noticed that the sensitivity and detection range of the biosensor preceded the majority of the existing methods for kanamycin which is due to the ETBR and bipedal DNA walker excellent signal amplification efficiency.

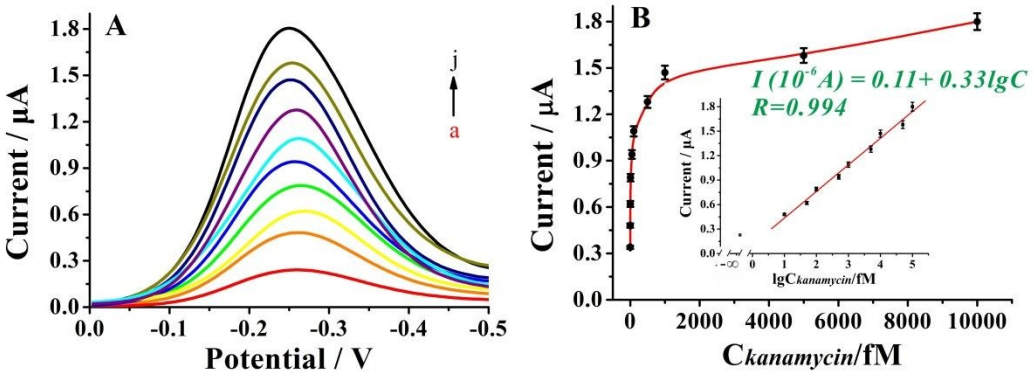

Fig.4. (A) DPV responses of our bipedal DNA walker toward kanamycin with different concentrations (from curve a-j: 0 pM, 10 fM, 50 fM, 100 fM, 500 fM, 1 pM, 5 pM, 10 pM, 50 pM, 100 pM respectively); (B) Variance of DPV intensity as a function of kanamycin with various concentrations. Inset: the calibration curve of

Published on 11 February 2020. Downloaded by University of Newcastle on 2/12/2020 9:10:41 AM.

Analyst Accepted Manuscript

View Article Online
DOI: 10.1039/D0AN00139B

DPV peak current versus the logarithm of kanamycin in range from 0 to 100 pM. Error bars showed the standard deviations across three repetitive experiments.

Table 2. Comparison of different assay strategies for kanamycin determination.

Detection method	Detection range	Detection limit	Reference
ELISA	1.7 pM-3.4 pM	7.7 pM	34
HPLC	10 nM-150 nM	25 nM	35
SERS	1 nM-100 nM	0.75 nM	36
SPR	100 nM-10 μM	43 nM	10
Colorimetry	50 pM-500 pM	14.7 pM	13
Fluorescence	24.75 nM-137.15 nM	7.5 nM	37
Luminescence	0.2 μM-150 μM	14.3 nM	38
Electrochemistry	1 nM to 10 mM	1 nM	39
Electrochemistry	1 pM to 10 nM	0.5 pM	40
Electrochemistry	10 fM-100 pM	7.1 fM	This work

3.6 Detection Specificity of the bipedal DNA machine

To evaluate the specificity of our strategy for the kanamycin assay, the electrochemical biosensor was challenged with target kanamycin and other non-target antibiotics containing ampicillin, streptomycin, oxytetracycline, tobramycin and

Published on 11 February 2020. Downloaded by University of Newcastle on 2/12/2020 9:10:41 AM.

Analyst Accepted Manuscript

View Article Online
DOI: 10.1039/D0AN00139B

terramycin. The results were shown in **Fig.5**. The DNA machine only exhibited a strong DPV response in the presence of kanamycin, while the current response to several non-target antibiotics caused extremely weak current intensities. These results distinctly proved the excellent specificity of our sensing platform for the kanamycin detection.

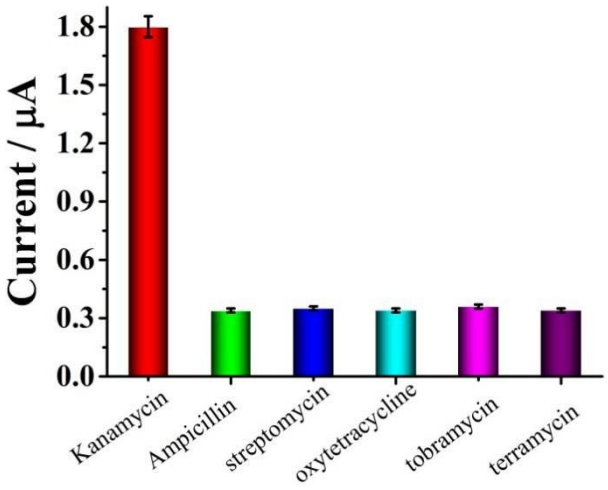

Fig.5. DPV responses acquired of the DNA machine for different antibiotics detection. The concentration of kanamycin was 100 pM, other non-target antibiotics were 1 nM. Error bars were standard deviations across three repetitive experiments.

3.7 Real sample analysis

To test the applicability of our biosensor, the quantitative assay of kanamycin in drinking water was performed. Various concentrations of kanamycin were added into the drinking water samples and measured without pretreatment except for dilution with the reaction buffer. As shown in **Table 3**, these results obtained by our strategy were approximate to spiked amount, the recovery of the proposed strategy was in the

Published on 11 February 2020. Downloaded by University of Newcastle on 2/12/2020 9:10:41 AM.

Analyst Accepted Manuscript

View Article Online
DOI: 10.1039/D0AN00139B

range of 95.5% to 105.7%. These data clearly revealed the bipedal DNA machine could hold a great promise for real sample analysis with a desirable reliability and accuracy.

Table 3 Application of the DNA machine to detect kanamycin in drinking water.

Spiked amount (fM)	Measured amount (fM)	Recovery (%) ± SD, n=5
1.00×10^{1}	$(1.032\pm0.012)\times10^{1}$	103.2±1.2
1.00×10^{2}	$(1.042\pm0.015)\times10^{2}$	104.2±1.5
1.00×10^{3}	$(1.010\pm0.042)\times10^{3}$	101.0±4.2
1.00×10^{4}	$(1.013\pm0.041)\times10^{4}$	101.3±4.1
1.00×10^{5}	$(0.969\pm0.014)\times10^{5}$	96.9±1.4

4. Conclusion

In summary, we develop an Exonuclease III-aided target-aptamer binding recycling (ETBR) activated bipedal DNA machine for ultrasensitive electrochemical detection of antibiotic. As far as we know, this is the first time that bipedal DNA machine has been integrated into electrochemical sensing for antibiotics. Benefiting from ETBR and efficient strand displacement amplification provided by bipedal DNA walker, our electrochemical biosensor achieves improved sensitivity with a detection limit as low as 7.1 fM. Furthermore, the bipedal DNA machine surpasses conventional single swing arm DNA machine in terms of walking efficiency and

Published on 11 February 2020. Downloaded by University of Newcastle on 2/12/2020 9:10:41 AM.

Analyst Accepted Manuscript

View Article Online
DOI: 10.1039/D0AN00139B

stability. Therefore, this purposed electrochemical platform indeed offers an ingenious and practical method for sensing of antibiotics residues and related food safety analysis.

Acknowledgements

This work was supported by National Natural Science Foundation of China (31471644), the Primary Research & Development Plan of Shandong Province (2017GSF220009), program for Taishan Scholar of Shandong provinces (ts201712048).

References

1. A. Sharma, G. Istamboulie, A. Hayat, G. Catanante, S. Bhand and J. L. Marty, *Sensor Actuat B: Chem*, 2017, **245**, 507-515.

2. B. Wang, X. L. Lv, D. Feng, L. H. Xie, J. Zhang, M. Li, Y. Xie, J. R. Li and H. C. Zhou, *J Am Chem Soc*, 2016, **138**, 6204-6216.

3. X. He, Y. Xu, J. Chen, J. Ling, Y. Li, L. Huang, X. Zhou, L. Zheng and G. Xie, *Water Res*, 2017, **124**, 39-48.

4. J. Liu, J. Zeng, Y. Tian and N. Zhou, *Analyst*, 2017, **143**, 182-189.

5. L. Chiesa, S. Panseri, E. Pasquale, R. Malandra, R. Pavlovic and F. Arioli, *Food Chem*, 2018, **258**, 222-230.

6. Y. Zhai, Y. Zheng, Z. Ma, Y. Cai, F. Wang, X. Guo, Y. Wen and H. Yang, *ACS Sens*, 2019, **4**, 2958-2965.

7. K. W. Chang, H. W. Cheng, J. Shiue, J. K. Wang, Y. L. Wang and N. T. Huang, *Anal Chem*, 2019, **91**, 10988-10995.

Published on 11 February 2020. Downloaded by University of Newcastle on 2/12/2020 9:10:41 AM.

Analyst Accepted Manuscript

View Article Online
DOI: 10.1039/D0AN00139B

8. L. Zhou, Z. Liu, Z. Guan, B. Tian, L. Wang, Y. Zhou, Y. Zhou, J. Lei, J. Zhang and Y. Liu, *Appl Catal B-Environ*, 2020, **263**, 118326.

9. S. Kim and H. J. Lee, *Anal Chem*, 2017, **89**, 6624-6630.

10. L. Zhang, C. Zhu, C. Chen, S. Zhu, J. Zhou, M. Wang and P. Shang, *Food Chem*, 2018, **266**, 170-174.

11. J. Sun, A. R. Warden, J. Huang, W. Wang and X. Ding, *Anal Chem*, 2019, **91**, 7524-7530.

12. Y. Y. Wu, P. Huang and F. Y. Wu, *Food Chem*, 2020, **304**, 125377.

13. X. Cui, R. Li, X. Liu, J. Wang, X. Leng, X. Song, Q. Pei, Y. Wang, S. Liu and J. Huang, *Anal Chim Acta*, 2018, **997**, 1-8.

14. J. Zeng, N. Gan, K. Zhang, L. He, J. Lin, F. Hu and Y. Cao, *Talanta*, 2019, **199**, 491-498.

15. Y. Tang, C. Gu, C. Wang, B. Song, X. Zhou, X. Lou and M. He, *Biosens Bioelectron*, 2018, **102**, 646-651.

16. Q. Li, D. Zhou, J. Pan, Z. Liu and J. Chen, *Analyst*, 2018, **143**, 5670-5675.

17. R. Zhang, Y. Wang, X. Qu, S. Li, Y. Zhao, F. Zhang, S. Liu, J. Huang and J. Yu, *Analyst*, 2019, **144**, 4995-5002.

18. H. Wang, Y. Wang, S. Liu, J. Yu, W. Xu, Y. Guo and J. Huang, *Chem Commun*, 2015, **51**, 8377-8380.

19. H. Wang, Y. Wang, S. Liu, J. Yu, Y. Guo, Y. Xu and J. Huang, *Biosens Bioelectron*,2016, **80**, 471-476.

20. Q. Wu, H. Wang, K. Gong, J. Shang, X. Liu and F. Wang, *Anal Chem*, 2019, **91**, 10172-10179.

21. X. Chen, J. Wang, H. Y. Shen, X. Su, Y. Cao, T. Li and N. Gan, *ACS Sens*, 2019, **4**,

Published on 11 February 2020. Downloaded by University of Newcastle on 2/12/2020 9:10:41 AM.

Analyst Accepted Manuscript

View Article Online
DOI: 10.1039/D0AN00139B

2131-2139.

22. R. Zeng, L. Zhang, L. Su, Z. Luo, Q. Zhou and D. Tang, *Biosens Bioelectron*, 2019, **133**, 100-106.

23. W. Yang, Y. Shen, D. Zhang and W. Xu, *Chem Commun*, 2018, **54**, 10195-10198.

24. Y. Guo, Y. Wang, S. Liu, J. Yu, H. Wang, Y. Wang and J. Huang, *Biosens Bioelectron*, 2016, **75**, 315-319.

25. H. Fang, N. Xie, M. Ou, J. Huang, W. Li, Q. Wang, J. Liu, X. Yang and K. Wang, *Anal Chem*, 2018, **90**, 7164-7170.

26. Y. Zhang, X. Li, Z. Xu, Y. Chai, H. Wang and R. Yuan, *Chem Commun*, 2018, **54**, 10148-10151.

27. R. Zhang, Y. Wang, X. Qu, S. Li, Y. Zhao, S. Liu and J. Huang, *Sensor Actuat B: Chem*, 2019, **297**, 126771.

28. F. Yang, X. Zhong, X. Jiang, Y. Zhuo, R. Yuan and S. Wei, *Biosens Bioelectron*, 2019, **130**, 262-268.

29. J. Huang, L. Zhu, H. Ju and J. Lei, *Anal Chem*, 2019, **91**, 6981-6985.

30. Z. Chen, C. Wang, L. Hao, R. Gao, F. Li and S. Liu, *Biosens Bioelectron*, 2019, **128**, 104-112.

31. S. Cai, M. Chen, M. Liu, W. He, Z. Liu, D. Wu, Y. Xia, H. Yang and J. Chen, *Biosens Bioelectron*, 2016, **85**, 184-189.

32. W. Liu, A. Chen, S. Li, K. Peng, Y. Chai and R. Yuan, *Anal Chem*, 2019, **91**, 1516-1523.

33. J. Yang, B. Dou, R. Yuan and Y. Xiang, *Anal Chem*, 2017, **89**, 5138-5143.

34. J. He, Y. Wang and X. Zhang, *Food Anal Method*, 2015, **9**, 744-751.

35. B. Blanchaert, E. Poderós Jorge, P. Jankovics, E. Adams and A. Van Schepdael, *Chromatographia*, 2013, **76**, 1505-1512.

Published on 11 February 2020. Downloaded by University of Newcastle on 2/12/2020 9:10:41 AM.

Analyst Accepted Manuscript

View Article Online
DOI: 10.1039/D0AN00139B

368 36. A. H. Nguyen, X. Ma, H. G. Park and S. J. Sim, *Sensor Actuat B: Chem*, 2019, **282**,
369 765-773.

370 37. S. Dehghani, N. M. Danesh, M. Ramezani, M. Alibolandi, P. Lavaee, M. Nejabat, K.
371 Abnous and S. M. Taghdisi, *Anal Chim Acta*, 2018, **1030**, 142-147.

372 38. K.-H. Leung, H.-Z. He, D. S.-H. Chan, W.-C. Fu, C.-H. Leung and D.-L. Ma, *Sensor*
373 *Actuat B: Chem*, 2013, **177**, 487-492.

374 39. R. Liu, Z. Yang, Q. Guo, J. Zhao, J. Ma, Q. Kang, Y. Tang, Y. Xue, X. Lou and
375 M. He, *Electrochimica Acta*, 2015, **182**, 516-523.

376 40. C. Han, R. Li, H. Li, S. Liu, C. Xu, J. Wang, Y. Wang and J. Huang,
377 *Microchimica Acta*, 2017, **184**, 2941-2948.

Published on 11 February 2020. Downloaded by University of Newcastle on 2/12/2020 9:10:41 AM.

Analyst Accepted Manuscript